Measurement of the particle number density in a pulsed flow gas cell with a second-harmonic interferometer

IOP Conf. Series: Journal of Physics: Conf. Series **1079** (2018) 012006 doi:10.1088/1742-6596/1079/1/012006

Measurement of the particle number density in a pulsed flow gas cell with a second-harmonic interferometer

F Brandi[1,2], P Marsili[3], F Giammanco[3], F Sylla[4] and LA Gizzi[1]

[1] Intense Laser Irradiation Laboratory (ILIL), Istituto Nazionale di Ottica (CNR-INO), Via Moruzzi 1, 56124 Pisa, Italy
[2] Istituto Italiano di Tecnologia (IIT), Via Morego 30, 16163 Genova, Italy
[3] Dipartimento di Fisica, Università degli Studi di Pisa, Largo B. Pontecorvo 3, 56127 Pisa, Italy
[4] SourceLAB SAS, 86 rue de Paris, 91400 Orsay, France

E-mail: `fernando.brandi@ino.cnr.it`

Abstract.
A high-sensitivity high-speed second-harmonic interferometer is used to monitor the particle number density inside a pulsed flow gas cell designed for laser wakefield acceleration. The interferometer can precisely follow the particle density temporal evolution therefore offering a practical way to control in real-time the target density during laser-plasma interaction. The presented results are relevant for the evaluation of density diagnostic tools for flow gas cells used as laser-plasma acceleration stages.

1. Introduction

The demonstration of laser wakefield acceleration (LWFA) of electrons to the GeV level [1, 2] opens the way for the application of LWFA-based accelerators and high photon energy radiation sources [3] within user oriented facilities with superior beam quality and reliability necessary for actual high-level applications, as envisaged within the EuPRAXIA project [4]. The transition from fundamental research to actual implementation must go along with a full control and tailoring of the laser-plasma based accelerator, and specifically of the plasma free-electron density. In LWFA the plasma in the gas target is created either by the laser pulse itself or pre-generated by an electric discharge or by a second laser pulse.

Gaseous targets used in LWFA are: *i) supersonic gas jets* that are easy to implement, allow for a good control over the peak particle number density [5], but produce density profiles that can vary shot-to-shot due to reproducibility of valve operation over time and turbulent flow, and prevent high repetition rate operation due to pulsing capability. *ii) Capillary discharges* that provides guiding of the laser up to centimeters, thus increasing the acceleration length [1], but can get damaged during usage and may require somehow sophisticated density diagnostics methods [6] which pose technical challenges; *iii) flow gas cells* that are very good candidates to avoid the above mentioned limitations, allowing for a stable and controllable laser-plasma interaction even at high repetition rate along with easily tunable accelerator length [7–14]. Flow gas cells are also suitable to be implemented in multi-stage accelerators [15, 16], which

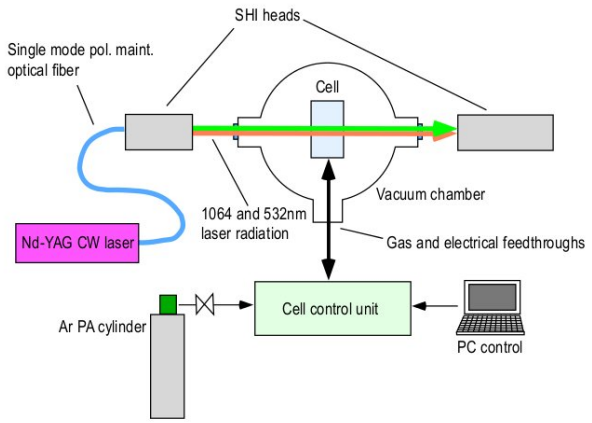

Figure 1. Schematic of the experimental apparatus.

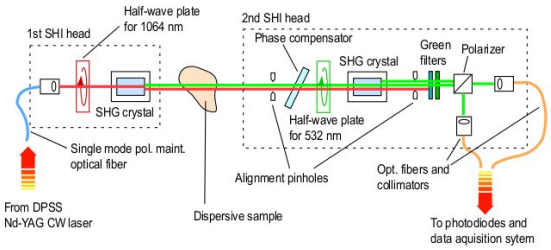

Figure 2. Schematic of the second-harmonic interferometer.

is important in the perspective of designing and implementing LWFA-based facilities. In this context the reliable and robust measurement and control of the free-electron density is a crucial aspect, and interferometry plays a major role as diagnostic tool being non-invasive and versatile. Typical two-arm interferometers [17] suffer from a high sensitivity to environmental conditions which limits their use outside the laboratory environment. Nomarski and folded two-arm interferometers provide better stability compared to standard two-arm interferometers, are widely used in research laboratories [18–21], and provide an interferogram from which the phase is retrieved applying image analysis software and phase-unwrapping algorithms. The lengthy data analysis limit their use in real-time measurements, while they may be suitable for off-line measurements during alignment and tuning of the laser-plasma accelerator stages.

When stability and ease of implementation matters, an alternative robust interferometric method is the second-harmonic interferometer (SHI), also called dispersion interferometer [22]. The SHI is a single-arm, two-color interferometer, which is sensitive to the change of refractive index between the fundamental and second-harmonic wavelength, measured phase shift given by $\Delta\phi = \frac{4\pi}{\lambda}\int_L \Delta n(\lambda)dl = \frac{4\pi}{\lambda}L\overline{\Delta n}(\lambda)$, where $\Delta n(\lambda) = n(\lambda) - n(\lambda/2)$, $n(\lambda)$ is the refractive index, λ is the wavelength, and L the optical path in the sample. Being a fully common-path interferometer the SHI is insensitive to vibration when compared with typical two-arm interferometers, which allows long term stable operation even in a harsh environment [23].

In this work, the latest results on the use of a high-speed ($\sim \mu$s) and high-sensitivity ($\sim$ mrad) SHI based on a CW Nd:YAG laser to measure the particle number density inside a pulsed flow gas cell in vacuum are presented.

2. Experiment

Fig.1 shows a schematic block diagram of the experimental apparatus. The cell (model SL-ALC, SourceLAB) is placed in a cylindrical vacuum chamber, evacuated by a turbo-molecular pump to 10^{-5} mbar. The gas cell comprises two 600 μm-diameter apertures to allow the gas to flow in the vacuum chamber, two lateral glass windows at $L = 35$ mm to enable transverse interferometry. When the gas pulse flows out of the cell the pressure in the chamber increases shortly, not exceeding however values of the order of 10^{-2} mbar. The vacuum chamber is equipped with three KF50 vacuum flanges on the lateral surface. Two lie opposite along a diameter and are used to mount BK7 optical precision windows, anti-reflection coated for 1064 nm and 532 nm wavelengths, providing entrance and exit of the interferometer beams. The third flange hosts the gas and electrical feedthroughs between the cell and the controller. The argon gas at 2

bar enters the control unit which then sends a gas puff to the cell at a pre-set pressure and duration. It is noted that if the cell would be continuously feed with gas or long gas pulses were used, the effect from back-ground density build up in the chamber would become visible during the interferometric measurement. Such effect was not revealed for the gas pressure and pulse length used. In case longer pulses and/or higher pressures would be needed the vacuum system (chamber plus pump) would have to be adequately scaled in order to avoid density build up in the interaction chamber.

Fig. 2 shows a detailed sketch of the fully fiber-coupled SHI interferometer used in the experiment [24–26], which is here briefly described. The radiation of a CW DPSS Nd-YAG laser is sent to the first interferometer head using a single mode polarization maintaining optical fiber. The laser light emerging from the fiber is collimated to a diameter of 1 mm. A half-wave plate is used to adjusts the polarization, in order to ensure an optimal harmonic generation in the first type-I SHG crystal. Both the 1064 nm and 532 nm beams leave the first head and are sent collinearly thought the cell. In the cell the two components suffer a de-phasing due to the gas dispersion and proportional to the gas number density. The transmitted beams enter the second head where a half-wave plate rotates the second-harmonic polarization by an angle of 90° leaving the fundamental beam polarization unchanged. A tilted glass slab adds a controlled de-phasing acting as a compensator, in order to tune the phase difference to an optimal working point. In a second type-I SHG crystal the 1064 nm beam is duplicated again. Following the filtering out of the residual 1064 nm beam, the two 532 nm beams with crossed polarizations enters a polarizing cube oriented by an angle of 45°, where the two beams are mixed giving rise to two complementary interference patterns. The beams emerging from the beam-splitter cube are finally collected by two fiber optic cables and sent to photodiodes, directly connected to ultra low-noise transimpedance amplifiers. The output signals are acquired by a 15 MHz USB digitizing oscilloscope controlled by a labview software which calculates in real-time the ratio between the difference and the sum of the digitalized signals. The recorded quantity is equal to $V\sin(\Delta\phi+\phi_0)+\alpha$ [24], where $\phi_0 \ll 1$ is the off-set phase that can be controlled acting on the phase compensator, V is the fringe visibility, and $\alpha \ll 1$ is related to the detector responsivities. The visibility is directly obtained by scanning the phase compensator over half-fringe [25, 27] and it is $V = 0.9$.

3. Results

The Gladstone-Dale relation between the refractive index n and the number density N, i.e., $(n-1) \propto N$, is used to obtain the particle number density from the measured phase by the equation $\overline{N} = \frac{\lambda}{4\pi L}\frac{N_0}{\Delta n_0}\Delta\phi = 1.63\Delta\phi \times 10^{19}$ cm^{-3}, where $N_0 = 2.69\times10^{19}$ cm^{-3} is the Loschmidt constant and $\Delta n_0 = 4\times10^{-6}$ the difference of the refractive index of argon at 1064 nm and 532 nm [28].

The results of the systematic measurements for a 100 ms gas pulse at various values of the pre-set backing pressure are reported in Fig. 3. The zero point represent the time when the trigger is sent to the cell's controller. In less then 100 ms from the trigger the filling up of the cell starts and lasts for about 100 ms. Then the gas density in the cell drops exponentially with a decay time of ∼0.9 s.

In Fig. 4 a comparison between 100 ms and 500 ms long gas pulses is shown for two values of the backing pressure. As expected the filling up of the cell lasts longer for the longer gas pulse and the achieved peak density value is larger by a factor ∼1.5.

Fig. 5 shows the values of the peak density value obtained in the experimental conditions investigated, while the dashed-line indicate the density estimated from the ideal gas law at the preset backing pressure and ambient temperature, reported as reference.

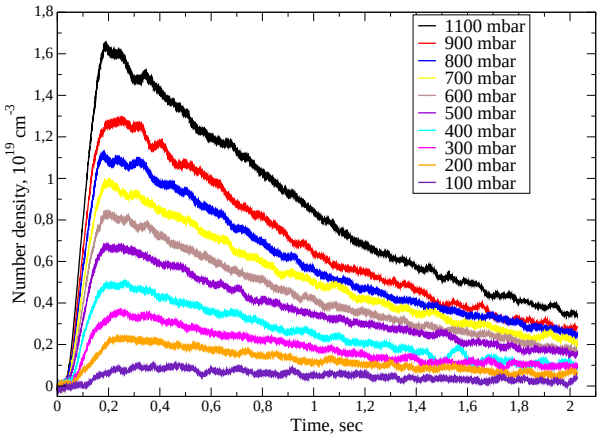

Figure 3. Time evolution of the average particle number density for a 100 ms gas pulse at various backing pressure settings.

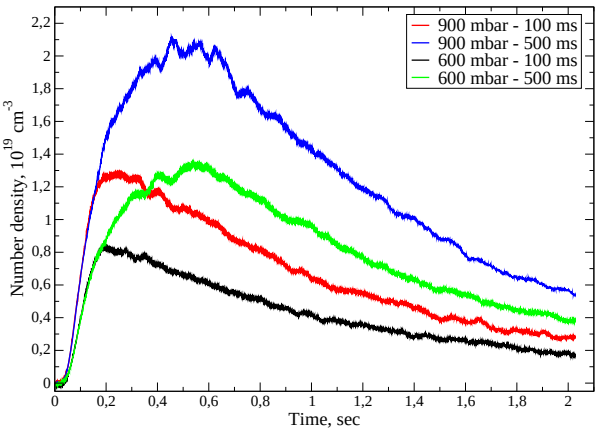

Figure 4. Time evolution of the average particle number density for a 100 ms and 500 ms gas pulse at two backing pressure settings.

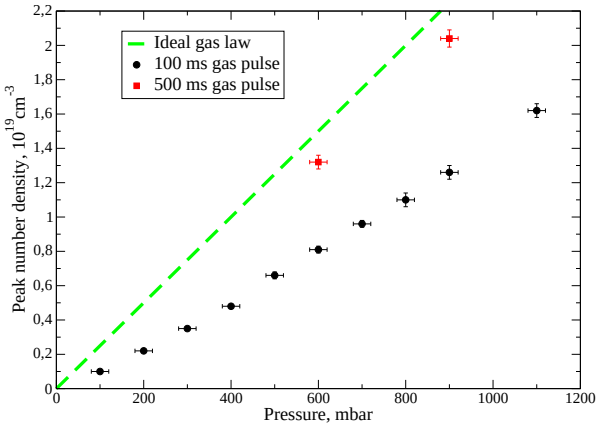

Figure 5. Peak value of the particle number density for 100 ms and 500 ms gas pulse at various backing pressure settings.

4. Conclusions

A second-harmonic interferometer is used to monitor in real-time the particle number density in a commercial pulsed flow gas cell designed for LWFA. It is found that diagnostic method is successful in measuring the density temporal evolution inside the cell from the filling up to the evacuation in the range up to 10^{19} cm^{-3}. The achieved peak value is less then what estimated from the ideal gas law especially for the shortest gas pulse, therefore characterization and continuous monitoring of the gas density is necessary in order to tune and control the laser-plasma interaction process inside the cell. The experiment performed and the results obtained are important towards the implementation of gas cells as laser-plasma based acceleration stages in a fully controlled and user oriented particle accelerator facility, as that envisaged within the EuPRAXIA design study project.

It is noted that the SHI presented can be used also to measure the particle density for other gases typically used in LWFA, like H_2 and He. The difference between the refractive indices at 1064 nm and 532 nm in hydrogen and helium at STP are 2.8×10^{-6} and 2.2×10^{-7} respectively [28]. Therefore, the measurement can be performed with hydrogen instead of argon. In case of helium, the expected phase shift at STP is ∼90 mrad, therefore the SHI with a noise level down to less the 1 mrad [24] is capable of measuring He number density within the cell in the order of 10^{17} cm^{-3}.

In perspective, the development of a 2D imaging version of the SHI would allow to monitor

samples with non-uniform and/or non-cylindrically symmetric spatial density distribution, like gas jets from square nozzles and/or with shock fronts. There are reports in the literature about 2D second-harmonic interferometry [29–31] however more research and development activity is necessary to validate the imaging SHI methodology as viable diagnostics for LWFA gas target.

Acknowledgments
FB and LG acknowledge the financial support from the European Unions Horizon 2020 research and innovation programme Grant Agreement No 653782 EuPRAXIA, and from the Istituto Italiano di Tecnologia (convenzione operativa IIT CNR-INO prot. n. 0010983, 26/11/2013).

References

[1] Leemans W P *et al.* 2014 Multi-GeV Electron Beams from Capillary-Discharge-Guided Subpetawatt Laser Pulses in the Self-Trapping Regime *Phys. Rev. Lett.* **113** 245002
[2] Hyung T K *et al.* 2017 Stable multi-GeV electron accelerator driven by waveformcontrolled PW laser pulses *Sci. Rep.* **7** 10203
[3] Gizzi L A *et al.* 2009 An integrated approach to ultraintense laser sciences: The PLASMON-X project *Eur. Phys. J. Spec. Top.* **175** 3-10
[4] Walker P A *et al.* 2017 Horizon 2020 EuPRAXIA design study *J. Phys.: Conf. Ser.* **874** 012029
[5] Brandi F and Giammanco F 2011 Temporal and spatial characterization of a pulsed gas jet by a compact high-speed high-sensitivity second-harmonic interferometer *Opt. Express* **19** 25479–87
[6] Daniels J, Tilborg J van, Gonsalves A J, Schroeder C B, Benedetti C, Esarey E and Leemans W P 2015 Plasma density diagnostic for capillary-discharge based plasma channels *Phys. Plasmas* **22** 073112
[7] Osterhoff J *et al.* 2008 Generation of Stable, Low-Divergence Electron Beams by Laser-Wakefield Acceleration in a Steady-State-Flow Gas Cell *Phys. Rev. Lett.* **101** 085002
[8] Corde S *et al.* 2013 Observation of longitudinal and transverse self-injections in laser-plasma accelerators *Nature Comm.* **4** 1501
[9] Aniculaesei C, Kim H T, Yoo B J, Oh K H and Nam C H 2018 Novel gas target for Laser Wakefield Accelerators *Rev. Scient. Intrum.* **89** 025110
[10] Kononenco O *et al.* 2016 2D hydrodynamic simulations of a variable length gas target for density down-ramp injection of electrons into a laser wake field accelerator *Nucl. Instr. Meth. Phys. A* **829** 125-9
[11] Audet T L *et al.* 2016 Electron injector for compact staged high energy accelerator *Nucl. Instr. Meth. Phys. A* **829** 304-8
[12] Lee P, Maynard G, Audet T L, Cros B, Lehe R and Vay J-L 2016 Electron injector for compact staged high energy accelerator*Phys. Rev. Accel. Beams* **19** 112802
[13] Audet T L *et al.* 2016 Investigation of ionization-induced electron injection in a wakefield driven by laser inside a gas cell *Phys. Plasmas* **23** 023110
[14] Vargas M *et al.* 2014 Improvements to laser wakefield accelerated electron beam stability, divergence, and energy spread using three-dimensional printed two-stage gas cell targets *Appl. Phys. Lett.* **104** 174103
[15] Pollock B B *et al.* 2011 Demonstration of a narrow Energy Spread, $\sim$ 0.5 GeV Electron Beam from a Two-stage Laser Wakefield Accelerator *Phys. Rev. Lett.* **107** 045001
[16] Liu J S *et al.* 2011 All-Optical Cascaded Laser Wakefield Accelerator Using Ionization-Induced Injection *Phys. Rev. Lett.* **107** 035001
[17] Gizzi L A *et al.* 2006 Femtosecond interferometry of propagation of a laminar ionization front in a gas *Phys. rev. E* **74** 036403
[18] Feister S, Nees J A, Morrison J T, Frische K D, Orban C, Chowdhury E A and Roquemore W M 2014 A novel femtosecond-gated, high-resolution, frequency-shifted shearing interferometry technique for probing pre-plasma expansion in ultra-intense laser experiments *Rev. Scient. Intrum.* **85** 11D602
[19] Park J, Baldis H A and Chen H 2016 The implementation and data analysis of an interferometer for intense short pulse laser experiments *High Power Laser Science and Engineering* **4** E26, doi:10.1017/hpl.2016.21
[20] Kalal M, Slezak O, Martinkova M and Rhee Y J 2010 Compact Design of a Nomarski Interferometer and Its Application in the Diagnostics of Coulomb Explosions of Deuterium Clusters *Journal of the Korean Physical Society* **56** 287-94
[21] Ruiz-Camacho J, Beg F N and Lee P 2007 Comparison of sensitivities of Moire deflectometry and interferometry to measure electron densities in z-pinch plasmas. *J. Phys. D: Appl. Phys.* **40** 2026-32
[22] Hopf F, Tomita A, and Al-Jumaily G 1980 Second-harmonic interferometers *Opt. Lett.* **5**, 386–8

[23] Brandi F, Giammanco F, Harris W S, Roche T, Trask E and Wessel F J 2009 Electron density measurements of a field-reversed configuration plasma using a novel compact ultrastable second-harmonic interferometer *Rev. Sci. Instrum.* **80** 113501
[24] Brandi F and Giammanco F 2007 Versatile second-harmonic interferometer with high temporal resolution and high sensitivity based on a continuous-wave Nd:YAG laser *Opt. Lett.* **32** 2327–29
[25] Brandi F and Giammanco F, 2008 Harmonic interferometry in the visible and UV, based on second- and third-harmonic generation of a 25 ps mode-locked Nd:YAG laser *Opt. Lett.* **33** 2071-73
[26] Brandi F, Giammanco F, Conti F, Sylla F, Lambert G and Gizzi LA 2016 Note: Real-time monitoring via second-harmonic interferometry of a flow gas cell for laser wakefield acceleration *Rev. Sci. Instrum.* **87** (8) 086103
[27] Brandi F, Marsili P and Giammanco F 2008 Compact high-speed high-sensitivity second-harmonic interferometer for electron density measurement in AIP conference proceedings: Burning plasma diagnostics, **988**, 132–5
[28] Velsko S P and Eimerl D 1986 Precise measurements of optical dispersion using a new interferometeric technique *Appl. Opt.* **25**, 1344–49
[29] Minoshirna K and Matsumoto H 1997 In-situ measurements of shapes and thicknesses of optical parts by femtosecond two-colour interferometry *Opt. Commun.* **138** 6-10
[30] Abraham E, Minoshima K and Matsumoto H 2000 Femtosecond laser-induced breakdown in water: time-resolved shadow imaging and two-color interferometric imaging *Opt. Commun.* **176** 441-452
[31] Jobes, F C and Bretz N L 1997 A prototype imaging second harmonic interferometer. *Rev. Scient. Intrum.* **68** 709